ELSEVIER

Agricultural and Forest Meteorology 115 (2003) 5–17

AGRICULTURAL AND FOREST METEOROLOGY

www.elsevier.com/locate/agrformet

Canopy element influences on resolved- and subgrid-scale energy within a large-eddy simulation

Roger H. Shaw [a,*], Edward G. Patton [b]

[a] *Department of Land, Air and Water Resources, University of California, Davis, CA 95616, USA*
[b] *The Pennsylvania State University, University Park, PA 16802, USA*

Accepted 26 June 2002

Abstract

Large-eddy simulations described here have included the effect of canopy drag through the depth of a plant canopy. Specifically, we have considered the simulation of flow through a forest. Drag forces enter the simulation with the inclusion of form and viscous drag forces in the momentum equation. In addition, we have carried a variable to represent the kinetic energy (KE) associated with the turbulent wakes behind canopy elements. Assigning typical dimensions to canopy drag elements and, hence, to the scale of wake turbulence, we have evaluated wake effects on the dissipation process and on subgrid-scale (SGS) energy arising from the cascade of resolved-scale energy. Despite the fact that the rate of conversion of resolved-scale kinetic energy to wake energy is large, and the observation that wake energy is comparable with SGS energy, an effective diffusivity for wake turbulence can be ignored when calculated from wake-scale kinetic energy and a length scale based on element dimension. Thus, it is unnecessary to carry a wake energy variable in the simulation. On the other hand, it is very important that the process of conversion of SGS energy to wake-scale energy be included in the simulation because the action of wakes is to enhance the dissipation of SGS energy. Viscous drag appears to be of little consequence, at least in our calculations where elements are considered as flat plates and fully exposed to the grid-averaged flow.
© 2002 Elsevier Science B.V. All rights reserved.

Keywords: Subgrid-scale energy; Wake turbulence; Canopy turbulence

1. Introduction

While recent tower and mast studies in agricultural crops and forests have yielded fascinating details of the structure of the turbulent aspects of air flow, field observations are necessarily limited with regard to documenting the three-dimensional aspects of the flow. The penetrable roughness of a plant canopy imposes direct and crucial influences on the mean and turbulent parts of the wind field. Field studies of canopy flow (e.g. Finnigan, 1979; Shaw et al., 1983) reveal features of the momentum exchange and turbulence structure that are quite dissimilar from typical wall shear layer flows. In particular, the correlation between streamwise and vertical velocities, r_{uw}, at the canopy top is usually substantially larger in magnitude, implying more efficient exchange of momentum.

Quadrant analyses (Finnigan, 1979; Shaw et al., 1983) show that the downward sweep of high momentum air provides a greater contribution to exchange than does the ejection of low momentum air, in contrast to surface layer flow over smoother terrain in which the two contributions are of similar magnitude, or in which ejections dominate (Raupach, 1981). The contrast between the pattern of turbulence away from

* Corresponding author. Tel.: +1-902-634-3019.
E-mail address: rhshaw@ucdavis.edu (R.H. Shaw).

0168-1923/02/$ – see front matter © 2002 Elsevier Science B.V. All rights reserved.
PII: S0168-1923(02)00165-X

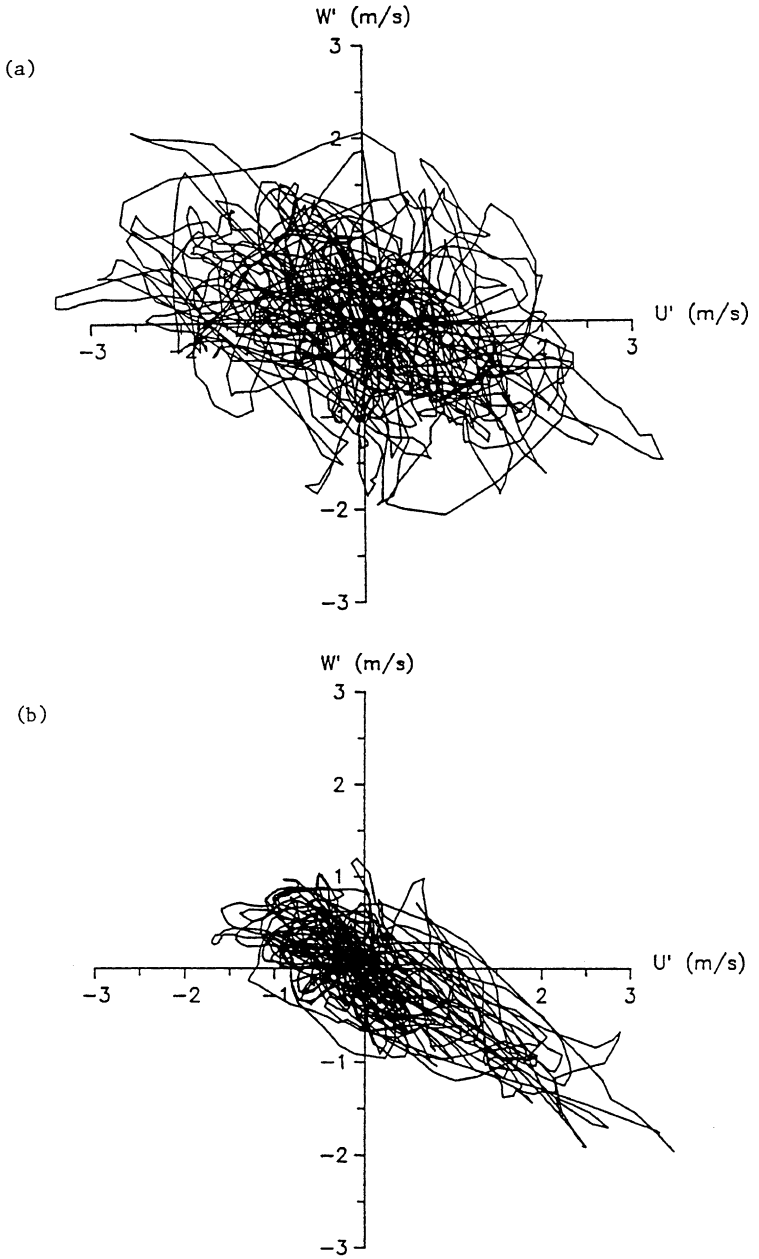

Fig. 1. Locus of the u', w' velocity perturbation during a 30 min period at the Camp Borden forest site at two heights: (a) 2.4 times treetop height, and (b) 0.86 times treetop height.

the canopy and in the vicinity of the top of the stand is illustrated clearly in Fig. 1, which shows a 30 min trace of the locus of the end point of the u', w' fluctuating velocity vector at two heights at a deciduous forest site (Shaw et al., 1988). Here, u and w refer to the streamwise and vertical velocity components and the primes designate a departure from the mean value. The u- and w-velocity signals near treetop level

exhibit substantially stronger correlation (correlation coefficient = −0.55) than those at twice the canopy height (correlation coefficient = −0.30), and contain an asymmetry not present at the higher level.

Such analyses provide a strong implication of structure to turbulence but yield no explicit information regarding spatial and temporal coherence. Micrometeorological studies of a forest by Denmead and Bradley (1985) were among the first to illustrate the presence of coherent flow structures that dominate the exchange process. The picture was further clarified by Gao et al. (1989) who presented a streamwise-sectional view of an ejection/sweep structure by invoking Taylor's hypothesis and inferring the streamwise spatial pattern from time traces of a vertical array of sonic anemometer/thermometers in a deciduous forest. A sloping scalar microfront appears at the interface between a downwind ejection of low momentum air from within the forest, and an upwind sweep of high momentum air.

Without concurrent information in the lateral direction, no inference can be made about the three-dimensional and vorticular properties of canopy turbulence. Likewise, without the ability to follow structures as they are carried by the flow, no information is gained about the temporal evolution of coherent structures. This provided the impetus to apply numerical procedures in an attempt to mimic observed canopy turbulence. Large-eddy simulation has been a valuable computational tool for the investigation of numerous geophysical flow scenarios. The technique has also been successful in replicating the main features of canopy flow (Shaw and Schumann, 1992; Su et al., 1998), both statistically and in terms of reproducing ejection/sweep patterns and scalar microfronts. However, questions remain with regard to the treatment in LES of the dynamical influence of individual canopy elements in transferring kinetic energy (KE) to scales comparable to element dimensions and, to date, such processes have been handled in a rather ad hoc fashion (Shaw and Schumann, 1992; Kanda and Hino, 1994).

Since, in general, individual elements of the canopy are not directly resolved by the numerical grid array, drag effects must be parameterized. Thus, in the resolved-scale momentum equation, the influence of the canopy elements appears as a drag force constructed from an element area density, a drag coefficient, and the local instantaneous velocity. Leaves and branches also create small-scale turbulence in their wakes. An important question arises regarding this wake-scale turbulence in a large-eddy simulation. Is its main action to contribute to the pool of subgrid-scale (SGS) energy, or does it have the overall effect of enhancing kinetic energy dissipation and reducing both SGS and resolved-scale energy? How wake turbulence is treated will strongly influence SGS energy within such numerical simulation, and will establish the relative importance of resolved-scale and SGS processes within the canopy. We discuss these issues and present results of a set of simulations aimed at estimating the contributions of wake-scale effects to canopy turbulence.

2. Wake turbulence and the unresolved scales

Proper treatment of spatial averaging in the formulation of the set of first and second-moment equations that govern canopy flow (Wilson and Shaw, 1977; Raupach and Shaw, 1982; Finnigan, 1985) results in the appearance of a form drag term in the turbulent kinetic energy (TKE) equation that represents the conversion of mean flow kinetic energy to wake-scale energy. Shaw and Seginer (1985) presented a framework for discussion of the influence of wakes on Reynolds-averaged TKE, and arrived at the conclusion that turbulence created in the wakes of plant elements is of sufficiently small-scale that it dissipates rapidly, effectively short-circuiting the inertial cascade process. Wilson (1988) expanded on this concept in the formulation of a higher-order closure model of flow through vegetation, in which separate equations were carried for turbulence created by large-scale shear and small-scale turbulence generated in element wakes. Turbulent motions are themselves impeded by drag elements and there is a spectral transfer of the kinetic energy of large-scale turbulence to that associated with wake-scale motions. Thus, distributed drag elements within a canopy accelerate the dissipation process.

Computational turbulence in a large-eddy simulation is classified as either resolved-scale or subgrid-scale, where band separation is set by the filter choice. In our simulation, we do not explicitly filter in the vertical direction and thus the band separation in this direction is defined by the grid dimension. For example,

with 10 grid levels through the depth of the canopy, *h*, the smallest resolved-scale of motion has a dimension of 0.2 h. On the other hand, typical canopy elements can be two orders of magnitude smaller again. In the simulation we present here, which is intended to represent a 20 m tall forest, a wavelength of 4 m separates resolved and SGS motions, while the characteristic dimension of individual elements of the canopy might be only 0.1 m. In general, the only aspect of plant distribution treated explicitly is the one-dimensional vertical profile of leaf and branch area density.

Wake-scale energy is clearly subgrid-scale, and it is important to evaluate its contribution to SGS energy. It can be readily shown that very substantial amounts of kinetic energy are transformed into wake scales as the mean and turbulent parts of the resolved-scale flow perform work against drag elements (Raupach and Shaw, 1982). It might not be immediately clear how to treat turbulence at this scale. One option would be to combine it with SGS energy arising through the action of SGS viscosity on resolved-scale shear in a cascade process. The problem this presents is the potential disparity in scales between energy arising from the two sources. One could imagine similar contributions to the kinetic energy in unresolved scales from inertial cascade and from wake motions but the much smaller wake scales would contribute much less to SGS viscosity, and the energy at the wake scales would dissipate much more quickly. By holding wake-scale energy as a separate energy pool in our large-eddy simulation, we are able to evaluate the magnitudes of terms in the budgets of the various kinetic energy pools, the relative contributions to total kinetic energy, and the relative importance of different scales to the diffusion process.

We discuss the impact of drag elements within a large-eddy simulation. Such simulation includes the shear production of turbulent kinetic energy that arises automatically within the simulation due to the dynamic instability of the computed flow field (there is no explicit treatment of resolved-scale TKE, as in an ensemble average "closure" model). LES incorporates the spectral transfer of resolved-scale TKE to SGS energy through the action of SGS eddy viscosity on the resolved-scale velocity shear. Viscous dissipation appears in the SGS energy equation and is parameterized according to the magnitude of SGS energy and a length scale normally set by the filter width. LES practitioners place much emphasis on the proper construction of SGS models with the simple Smagorinski model criticized for being too strongly dissipative, especially in the vicinity of boundaries and for not allowing backscatter (upscale transfer) of kinetic energy. While these criticisms are thought to be generally valid, we contend that for simulation of flow in penetrable roughness a more important consideration is the correct treatment of wake effects, since they are responsible for the spectral transfer of very large amounts of turbulent energy and are strongly dissipative.

3. Form and viscous drag forces

The presence of the canopy creates a balance of forces with drag appearing in the momentum equation. Drag consists of two components: (i) form or pressure drag, and (ii) viscous drag or skin friction. We are not aware of attempts to separate these two components in ensemble average models or in micrometeorological applications of LES. In fact, implicit in an acceptance of a constant element drag coefficient is the assumption that the obstruction to the flow is composed solely of form drag. We add a second component to the drag force in the momentum equation to represent viscous drag through a drag coefficient that is dependent on a drag element Reynolds number. The impact of such additional component of the drag is to increase the effective drag at low wind speeds but to have little impact at high speeds.

We assume that form drag is proportional to the square of the local wind speed, and that the Blasius relationship (Schlicting, 1968) holds for the skin friction component. A continuing problem in the specification of the drag coefficient for an element embedded within a foliage canopy is that the element usually lies within the shadow of upwind elements, and its effectiveness as a drag element may be substantially reduced. Thus, estimates of element drag coefficients based on calculations of momentum balance within canopies yield values that are considerably smaller than those deduced from exposure of individual elements in wind tunnels (Thom, 1971). To match observations in a deciduous forest (Shaw et al., 1988), we have selected a form drag coefficient of 0.15. To the form drag, we have added an

extra term to represent viscous drag in the following manner

$$F_i = -(C_d + C_{sf})\, a u_i V \quad (1)$$

where F_i is the drag force (per unit mass) in the x_i-direction, C_d a form drag coefficient, C_{sf} an equivalent coefficient to represent the effect of skin friction, a area density of drag elements, u_i the x_i-component of velocity, and V the total wind speed. Since viscous drag is not proportional to the square of the fluid velocity, the coefficient is not constant, as is C_d, but can be expressed as a function of a Reynolds number R_l based on element dimension ℓ_f and the local, instantaneous resolved-scale velocity. For flow over a flat plane oriented parallel to the flow, the Blasius solution for the skin friction coefficient is

$$C_{sf} = \frac{1.328}{\sqrt{R_l}} + \frac{2.326}{R_l} \quad (2)$$

However, for Reynolds numbers appropriate to leaves in tree canopies exposed to typical atmospheric flows, the second term on the right-hand side of this expression is at least an order of magnitude smaller than the first term, and we chose to neglect it. In our simulations, we have made no attempt to describe the canopy in terms of a spatial array of elements of different size, as would be found in a real stand of vegetation, but have assumed that a single element dimension is dominant.

The application of a coefficient, determined for a flat plate parallel to the flow, to leaves and branches in natural vegetation is questionable. However, potential errors are of opposite sign and to some extent self-canceling. Since leaves are not flat and are generally not oriented parallel to the flow, the drag coefficient is likely to overestimate skin friction. On the other hand, individual leaves are exposed to airflow substantially lower than the volume mean flow, suggesting that the coefficient should be higher. Without further guidance on this issue, we adopted the above expression as it stands. The net result of the addition of a constant form drag coefficient and a Reynolds number dependent skin friction coefficient is a combined drag coefficient/Reynolds number relationship of a form similar to that commonly used to represent the drag of cylinders or spheres (e.g. Schlicting, 1968), when compensation is made for the influence of aerodynamic shading.

4. Wake-scale kinetic energy

The action of element drag on airflow through the canopy is handled by the presence of the drag term F_i in the momentum equation. In terms of kinetic energy, the form drag component induces turbulence scales comparable to the individual drag elements (from both mean flow and resolved-scale turbulence). Opinions differ on how to treat such wake-scale KE. One option is to consider wake scales as comparable to the predominant subgrid-scales, in which case it is appropriate to consider wake production as a process contributing to SGS KE. The dissipation of such energy should then be treated in the traditional manner with a scale set by the filter width. On the other hand, if drag element dimensions are significantly smaller than the filter width, it is inappropriate to combine wake scale and SGS energy in the same category. The smaller scale wake turbulence should dissipate more quickly, and it is necessary to handle such kinetic energy separately.

Further, if there is a large disparity in scale between these two categories of unresolved motion, it would be appropriate to consider that SGS motions themselves interact with the canopy such that SGS energy cascaded from resolved-scales is further transformed into wake-scale KE (which dissipates relatively quickly). The latter idea led to the formulation of the SGS model in Shaw and Schumann (1992) in which no account was taken of the energy content of wake-scale motions, and in which a term was introduced to represent conversion of SGS energy to wake KE. This term acted in the SGS energy equation as an additional dissipation process.

Here, we carry separate conservation equations for SGS energy and wake-scale kinetic energy, acknowledging that wake-scale energy is also subgrid-scale. Each conservation equation includes all appropriate processes as identified in the schematic diagram of Fig. 2. This diagram is created in the style of Shaw and Seginer (1985) and Wilson (1988). In a Reynolds-average closure model, second-moment equations are carried for all turbulence scales but in a large-eddy simulation, turbulence evolves through a direct solution of the time-dependent Navier-Stokes equations and a budget for resolved-scale TKE is obtained diagnostically. Thus, in the simulation, there is no explicit separation of mean flow and

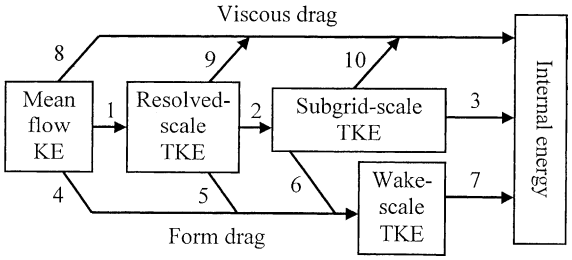

Fig. 2. Schematic of the processes that convert resolved-scale kinetic energy to subgrid-scale, wake scale, and ultimately to internal energy. Mean flow and resolved-scale turbulence are not treated explicitly but can be determined diagnostically from the LES output. Subgrid-scale and wake-scale turbulence are outputs of the LES. The numbers identify the various physical processes of energy exchange.

resolved-scale kinetic energy, as suggested by the diagram.

5. Subgrid-scale and wake-scale energy equations

The SGS energy equation takes its usual form, except that SGS energy is subject to the influences of form and viscous drag. Our simulation includes the integration of a prognostic equation for the SGS kinetic energy (Deardorff, 1980). With the above considerations, we write this equation in the form

$$\frac{\partial e}{\partial t} + \tilde{u}_i \frac{\partial e}{\partial x_i} = -\tau_{ij}\frac{\partial \tilde{u}_i}{\partial x_j} + \frac{\partial}{\partial x_i}\left(K_\mathrm{m}\frac{\partial e}{\partial x_i}\right) - \varepsilon - \varepsilon_\mathrm{fd} - \varepsilon_\mathrm{sf} \quad (3)$$

where the terms on the left-hand side are the local rate of change of SGS energy and the advective rate of change by the resolved-scale flow (as indicated by the tilde). In order of appearance on the right-hand side, terms represent: (i) energy cascade from resolved-scale to SGS, (ii) SGS and wake diffusion of SGS energy (K_m is diffusivity), (iii) free-air dissipation, (iv) enhanced dissipation in element wakes, and (v) direct dissipation in viscous-boundary layers.

The third term on the right ε is the dissipation that would occur in the absence of the vegetation elements. It is parameterized in the usual manner in the form

$$\varepsilon = \frac{c_\varepsilon e^{3/2}}{\ell_\Delta} \quad (4)$$

where ℓ_Δ, is a length scale set by the grid dimension, and is defined later (Eq. (9)). The coefficient c_ε is set to 0.93 according to Moeng and Wyngaard (1988). It can be argued (J.J. Finnigan, personal communication) that selected values of both c_ε and C_K (the latter to be defined later) are inappropriate for canopy flow, since Moeng and Wyngaard based their evaluation of the constants on the assumption of an inertial subrange with a slope of $-5/3$. Since energy is also extracted by canopy drag and the spectrum is expected to fall off more quickly, one should not anticipate the usual power law relationship. Nevertheless, in order to apply coefficients that retain constant values both in the free air above the canopy and within the vegetation elements, we accepted the Moeng and Wyngaard values.

The rate of conversion (ε_fd) of SGS kinetic energy to wake-scale kinetic energy is calculated as the work performed by SGS motion against form drag. It is obtained by first forming individual budgets for the grid-volume average variance of each SGS velocity component from the momentum equation with form drag included. On the assumptions that SGS turbulence is isotropic and non-skewed (to eliminate third moments), this energy transfer rate becomes

$$\varepsilon_\mathrm{fd} = \tfrac{8}{3} C_\mathrm{d} a \tilde{V} e \quad (5)$$

where $\tilde{V}$ is the magnitude of the resolved-scale velocity

$$\tilde{V} = (\tilde{u}^2 + \tilde{v}^2 + \tilde{w}^2)^{1/2} \quad (6)$$

and e is SGS kinetic energy. The procedure for obtaining this energy transfer rate is comparable, to that used in Wilson (1988), where the expression was applied to estimate the transfer of ensemble-average TKE to wake-scale energy. This additional dissipation term is also equivalent to that incorporated into the simulation of Shaw and Schumann (1992), who added a second loss term $-2e/\tau$ to the SGS energy equation to account for the effect of element wakes. Here, τ is a time scale for the drag that was set equal to $1/C_\mathrm{d} a \tilde{V}$. Thus, Shaw and Schumann (1992) included a term identical to ε_fd above but with a factor 2 rather than 8/3.

The action of skin friction is to make a direct transfer of SGS energy to internal energy. The effect is represented by the third dissipation term ε_sf formulated in a manner identical to that of ε_fd except with the Reynolds number dependent skin friction

drag coefficient C_{sf} substituted for constant form drag coefficient C_d.

An analogous expression is used to calculate wake-scale energy e_w, arising as a result of the form drag of canopy elements. We apply this in the following manner

$$\frac{\partial e_w}{\partial t} + \tilde{u}_i \frac{\partial e_w}{\partial x_i} = C_d a \tilde{V}^3 + \frac{8}{3} C_d a \tilde{V} e + \frac{\partial}{\partial x_i}\left(K_m \frac{\partial e_w}{\partial x_i}\right) - \varepsilon_w \quad (7)$$

where terms on the right represent, in order: (i) wake energy "production" as a result of form drag on the resolved-scale flow, (ii) transfer of SGS energy to wake-scale energy (ε_{fd} in the SGS energy equation), (iii) diffusion by SGS and wake-scale turbulence, and (iv) viscous dissipation of wake-scale energy. This latter is determined using the free-air formulation (as for dissipation of SGS energy) but with the length scale ℓ_f representative of canopy element dimension, such that

$$\varepsilon_w = \frac{c_\varepsilon e_w^{3/2}}{\ell_f} \quad (8)$$

The normally small dimension of canopy elements (relative to the grid size) would ensure the rapid dissipation of energy at these scales. In the extreme case that the element dimension matches the grid spacing, the impact of cascading energy from SGS to wake scale would be zero, since wake-scale energy would dissipate at the same rate as SGS energy. Strictly, Eq. (7) should include a term that represents the interaction of wake-scale motion with the viscous drag of downstream elements. Experience has shown that viscous drag effects on small-scale turbulence are negligible (see later discussion of Fig. 4), and we have chosen not to include this additional complication.

6. Subgrid-scale and wake-scale viscosity

In a large-eddy simulation, unresolved motions feed back to the resolved-scale flow through the action of a subgrid-scale viscosity. In the Deardorff (1980) version of this parameterization under neutral stability conditions, as used here, the viscosity is formulated from the SGS energy and a length scale ℓ_Δ, set by the grid dimension

$$\ell_\Delta = (1.5\Delta_x \times 1.5\Delta_y \times \Delta_z)^{1/3} \quad (9)$$

where the deltas are the grid dimensions. The factor 1.5 multiplying the x- and y-dimensions arises since we truncate the top one-third wavenumbers in these directions to eliminate aliasing errors introduced through spectral differencing, and to define the sub-filter scale. The numerical methods used to perform these simulations will be discussed further in Section 7. In the present situation, the viscosity must also include the contribution of wake-scale energy. It has been demonstrated to us (M.R. Raupach, personal communication) that the diffusivities of two uncorrelated turbulence fields are linearly additive, such that

$$K_m = C_K(\ell_\Delta e^{1/2} + \ell_f e_w^{1/2}) \quad (10)$$

where ℓ_f is a length scale set by the element dimension, and e_w is wake-scale kinetic energy. The coefficient C_K was set to 0.1 following Deardorff (1980) and Moeng and Wyngaard (1988).

The subgrid-scale Reynolds stress is estimated as the product of this SGS viscosity and the resolved-scale velocity shear such

$$\tau_{ij} = -K_m\left(\frac{\partial \tilde{u}_i}{\partial x_j} + \frac{\partial \tilde{u}_j}{\partial x_i}\right) \quad (11)$$

where $\tilde{u}_i$ is resolved-scale velocity. The divergence of this SGS Reynolds stress appears in the resolved-scale momentum equation. As stated earlier, this formulation has been criticized for being excessively dissipative and to result in near-wall wind profiles that do not match the expected semi-logarithmic form. However, the presence of a canopy creates an elevated shear zone where shear production is strongest, and the flow in the immediate vicinity of the lower boundary is of little consequence. In addition, canopy drag is the dominant dissipation process and details of SGS dissipation are believed to be of secondary importance.

7. Computational methods

The numerical method is based on the scheme of Moeng (1984) and Moeng and Wyngaard (1988) and integrates a set of three-dimensional, filtered Navier-Stokes equations under the Boussinesq approximation, with additional terms to represent form and viscous drag of canopy elements. A pseudospectral differencing technique is employed for horizontal derivatives,

and a second-order centered-in-space finite difference scheme determines vertical derivatives. To eliminate aliasing errors introduced by the pseudospectral technique applied in the horizontal directions, and to define the separation between resolved- and sub-filter scale motions, we impose a wave-cutoff filter by truncating the highest one-third wavenumbers. Incompressibility is forced by forming a Poisson equation for pressure from the divergence of the momentum equation. A third-order Runge-Kutta scheme is used to advance in time as in Sullivan et al. (1996). Periodic boundary conditions are imposed in the horizontal directions. Further details of the methodology may be found in Patton et al. (1998).

The domain comprises $96 \times 96 \times 30$ equally-spaced grid intervals in the *x*-, *y*- and *z*-directions. A vegetation canopy representing a 20 m tall forest occupies the lowest 10 grid points, with a vertical array of area density identical to that of Dwyer et al. (1997), and which integrates to a leaf area index (LAI) of 2.0. Flow is maintained by a domain-uniform driving force aligned in the *x*-direction such that the *y*, *z* cross-section average wind velocity equals 1 m/s. Thermally neutral conditions are preserved throughout all simulations. Runs were performed with values of ℓ_f equal to 0.05, 0.1, 0.2, 0.4, and 1.0 m.

Based on domain-averaged turbulent kinetic energy, equilibrium was reached after approximately 1000 time steps. For each run, 10 data sets were saved for analysis every 200 steps starting from 2200 and ending at the 4000-timestep point. Statistics were composed from these 10 time steps and from the 96×96 grid points in each horizontal plane. Time steps were variable but averaged 0.56 s. Thus, the period over which statistics were formed translates to a little over 1000 s in real time.

8. Results and discussion

The objective of this study has been to gauge the impact of canopy element drag on SGS energy,

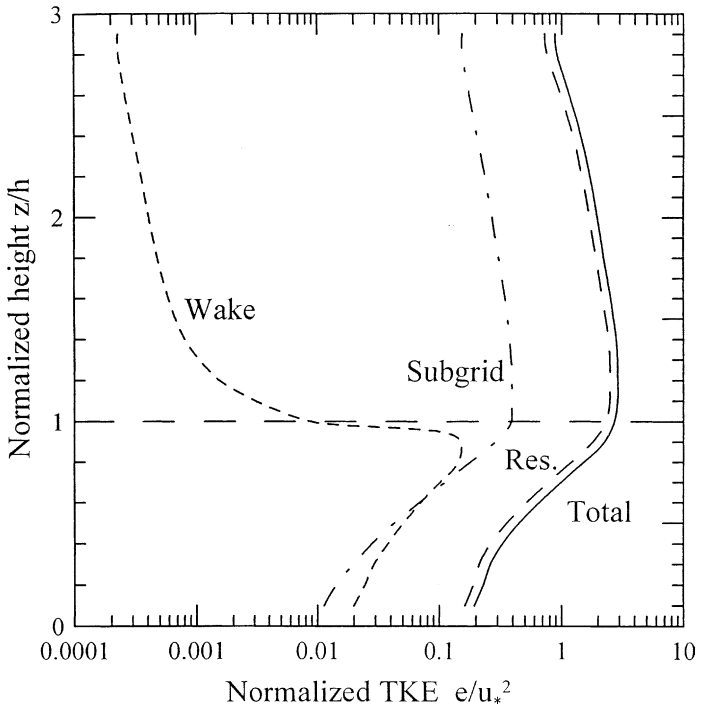

Fig. 3. Vertical profile of normalized turbulent kinetic energy normalized by u_*^2 (solid curve), and its constituents: (long dash line), resolved-scale flow field; (dash-dot line), SGS energy; (short dash line), wake-scale kinetic energy. Calculations were performed with an element dimension of 0.1 m.

and to evaluate the diffusive powers of wake-scale turbulence. To these ends, we present the contributions to turbulent energy of resolved-scale, SGS, and wake-scale energy, and the budgets of SGS energy and of wake-scale energy. We also compare the content of these two turbulent energy pools with resolved-scale turbulent kinetic energy, and compare the effective diffusivities of resolved-scale, SGS, and wake-scale energy.

Fig. 3 presents a vertical profile of turbulent kinetic energy and the three spectral components of which it is comprised. The TKE is normalized by the square of the friction velocity calculated from the Reynolds stress at the canopy top. It increases from the surface by an order of magnitude to reach a maximum value of about 3 just above treetop height. By far the largest contribution is that of the resolved-scale flow. The logarithmic scale allows us to examine in more detail the small contributions made by SGS and wake-scale energy. Within the canopy, each is a factor of about 10 smaller than the resolved-scale flow contribution.

Assigning a length scale of 0.1 m to the canopy elements, as in the case shown, results in SGS and wake-scale energy making roughly equal contributions through the depth of the forest. Wake-scale energy falls off quickly above treetop level, where it only remains above zero because of transport by the resolved-scale and SGS turbulence. The outcomes of runs with larger element scales are not shown. Basically, the results show little impact on the total TKE but progressively increasing contributions to TKE from wake scales until, with a dimension of 1 m, wake-scale kinetic energy in the middle and lower canopy makes as large a contribution as the resolved-scale flow field. The larger element scale does not affect the rate of production of wake-scale energy but reduces, in proportional manner, its rate of dissipation.

Fig. 4 shows a vertical profile of the terms in the budget of subgrid-scale energy for a foliage element dimension ℓ_f of 0.1 m. SGS motion gains kinetic energy from the action of SGS turbulence on resolved-scale shear, peaking at the canopy top with

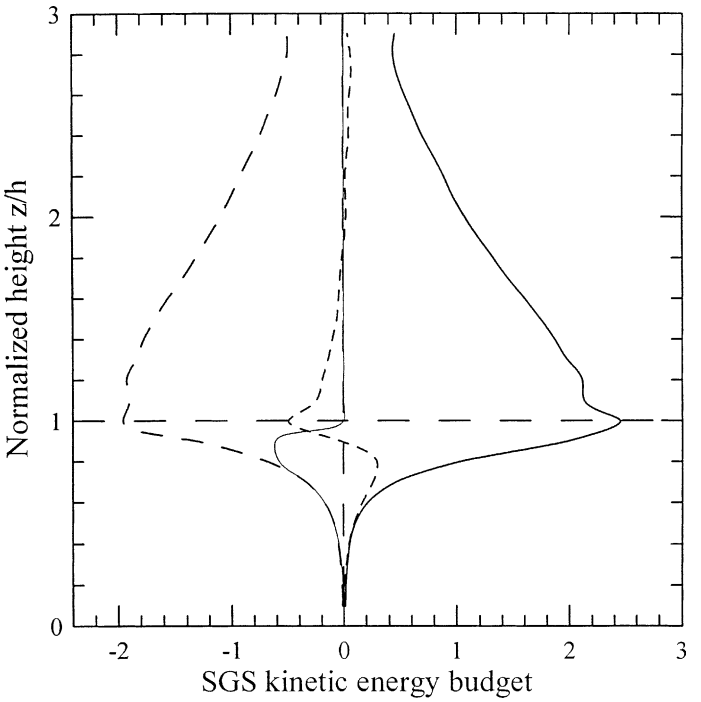

Fig. 4. Budget of SGS kinetic energy normalized by u_*^3/k: (heavy solid line), energy cascade from the resolved flow (process 2); (long dash line), SGS dissipation (process 3); (thin solid line), transfer of SGS energy to wakes (process 6); (short dash line), diffusion by resolved and subgrid-scale motions.

a magnitude of a little over a non-dimensional value of 2. Above the vegetation, viscous dissipation is the only sink of SGS energy. As seen, diffusion by both resolved and unresolved turbulence plays a relatively small role in distributing SGS energy in the vertical. Energy is removed from the upper layer of the canopy and the layer immediately above, and is carried into the canopy.

Within the canopy, canopy drag, through the formation of small-scale wakes, is an additional and equally important sink for kinetic energy. For the lowest three quarters of the canopy, free-air and wake dissipation rates are roughly the same magnitude. The near equality of the two dissipation processes is coincidental and a result of the selection of LAI. Were the LAI to be greater than the selected value of 2, wake dissipation would exceed free-air dissipation, and the opposite would be true if LAI < 2. Calculated values of the direct dissipation of SGS energy in the viscous-boundary layers of canopy elements were insignificant and are not shown in the figure. Similar calculations of the SGS energy budget were performed for each of the element dimensions considered but these are not presented because differences were relatively small. Only at the very largest element sizes (ℓ_f equal to 0.4 or 1.0 m) was there a noticeable change, with production and free-air dissipation both decreasing slightly in magnitude. Presumably, this is through the greater diffusivity of wake-scale energy causing a reduction in local resolved-scale shear.

The budget of turbulent energy associated with the wakes of canopy elements is illustrated in Fig. 5. The dominant terms are wake production due to the resolved-scale flow impinging on components of the vegetation, and viscous dissipation of this energy. The unresolved SGS motions naturally make a much smaller contribution to wake-scale energy. Again, element dimension has little impact on the budget. This is because the form drag force is not dependent on element size (see Eq. (1)). Viscous dissipation is a function of element size but wake-scale energy

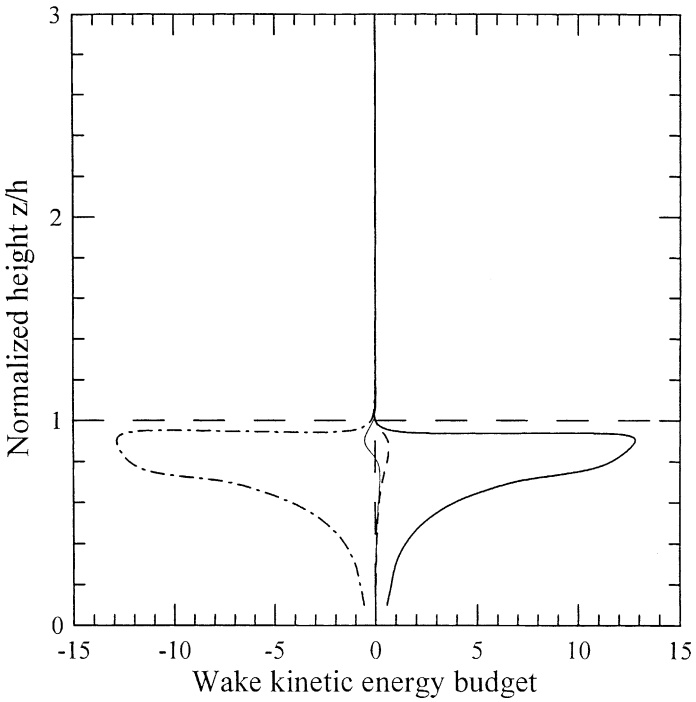

Fig. 5. Budget of wake-scale kinetic energy normalized by u_*^3/h: (heavy solid line), transfer of kinetic energy from the resolved flow in element wakes (processes 4 and 5); (dash-dot line), dissipation of wake-scale energy (process 7); (dash line), transfer of energy from SGS motions (process 6); (thin solid line), diffusion of wake-scale kinetic energy by resolved and subgrid-scale motions.

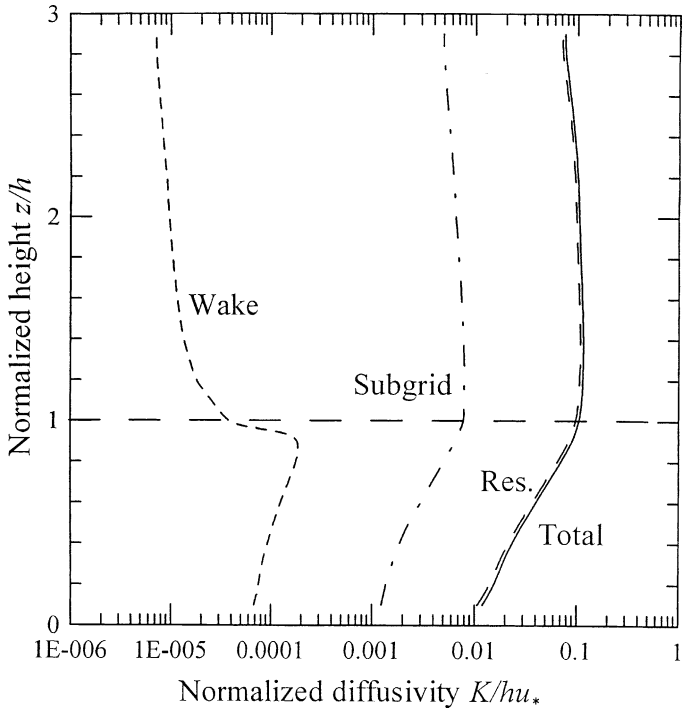

Fig. 6. Vertical profile of effective diffusivity and its components normalized by $u_* h$: (solid line), total diffusivity; (long dash line), resolved-scale component; (dash-dot line), component due to SGS motions; (short dash line), component due to wake-scale motions.

simply adjusts to an appropriate magnitude to force energy balance.

Finally, Fig. 6 shows vertical profiles of the effective diffusivities associated with resolved-scale, SGS and wake-scale turbulence. Again, only the case for a foliage element dimension ℓ_f of 0.1 m is shown. A diffusivity for the resolved-scale turbulence was calculated in a manner similar to that for SGS wake-scale turbulence (see Eq. (10)), using the same coefficient but a velocity scale based on resolved-scale TKE and a vertical length scale derived from two-point correlations presented in Su et al. (2000).

It is readily seen that the eddy diffusivity associated with resolved-scale turbulence is by far the largest of the three scales of motion. The contribution from SGS turbulence is an order of magnitude smaller and, in the canopy, wake-scale motions are an order of magnitude smaller again. The lack of significance of wake motions is a consequence of the relatively small physical dimension of the elements—diffusivity being the product of length and velocity scales. Only with the largest element dimensions used in the simulations does the diffusivity associated with wake motions become significant. This happens on two counts: the larger dimension and the larger turbulent velocity, as discussed earlier.

9. Summary and conclusions

Prior work has clearly demonstrated the value of large-eddy simulation as a tool for the examination of the turbulent nature of the air as it penetrates a plant canopy and conducts the exchange of a variety of vector and scalar quantities. Here, we have investigated an aspect of the flow that has a large impact on both the resolved and unresolved component of an LES flow field. That is, we have examined the contribution made by the wakes of canopy elements to subgrid-scale energy and diffusing power. Canopy elements create a transfer of kinetic energy from the mean flow to small-scale turbulence, and

are responsible for the scale conversion of turbulent kinetic energy from larger scales that are resolved within the LES, and from those classified as subgrid-scale.

To this end, we have added another variable to the simulation to represent the unresolved kinetic energy associated with the wakes behind canopy elements. This energy results from the action of form or pressure drag. Part of this energy is calculated directly in the simulation from the instantaneous, spatially varying resolved-scale flow field, while a second is estimated from the instantaneous, spatially varying SGS energy. Included in the simulations is the separation of form and viscous drag, and estimates of the direct dissipation of kinetic energy in the viscous-boundary layers surrounding each element.

A natural canopy is composed of a range of element types (trunks, branches, leaves, etc.) exhibiting an assortment of shapes and sizes. Furthermore, such elements are not uniformly distributed throughout the stand but tend to be clumped and exhibit varying density. None of these characteristics is treated here because of the need for economy in our numerical computations. Rather, our numerical "canopy" consists of a horizontally uniform array of element density, in which the elements themselves are spatially uniform in dimension, and their impact on the resolved and unresolved flow field are parameterized. We do attempt to represent a typical vertical variation in drag element area density.

As previously known, the creation of turbulent wakes behind canopy elements has the very large effect of transferring energy from the mean flow and from larger-scale turbulence to small-scales, which dissipate quickly. This process has been referred to as a "short circuit" of the normal, free-air inertial energy cascade. Our simulations confirm this action and also demonstrate the importance of considering the influence of wakes on kinetic energy classified within a large-eddy simulation as subgrid-scale. Considering that SGS energy in our simulation includes scales smaller than one-fifth of the canopy height (10 grid intervals representing the full depth of the canopy), and that most of this energy is present at the large-scale end of this range, wake scales in a typical vegetation canopy are at least one-order of magnitude smaller again. While drag effects on resolved energy are implicit through the inclusion of form and viscous drag in the momentum equation, the impact on SGS energy must be treated explicitly.

The rate of production of wake-scale kinetic energy is large but its small-scale ensures that it dissipates rapidly with the result that, with an element dimension of 0.1 m, the energy content of the wake-scales matches that of SGS energy within the canopy. On the other hand, the effective diffusivity of wake motions is small because this quantity is constructed from the product of turbulent velocity and length scales. We deduce, therefore, that it is not necessary to carry a variable to represent wake-scale energy in the simulation, as Wilson (1988) concluded in his higher-order closure model. However, the action of canopy elements on SGS energy, when element dimensions are an order of magnitude or more smaller than grid dimensions, is important and it is essential to include a term to represent this energy transfer in the SGS energy budget. Because canopy drag is strongly dissipative to the resolved-scale flow, it is proposed that, for LES of canopy flows, the nature of the SGS model employed is of secondary importance compared to the importance of SGS models in simulations of wall boundary layer flows.

Our calculations show the direct impact of viscous drag to be of little consequence both to the momentum equation and in terms of the direct dissipation of resolved-scale and SGS kinetic energy. A note of caution, though, is that we assumed viscous drag to be that of flat plates oriented parallel to the flow and to be fully exposed to the resolved-scale (grid-volume averaged) flow.

Acknowledgements

This study was supported by the National Science Foundation through award number ATM-0071377. Computer simulations relating to this work were performed on facilities at the National Center for Atmospheric Research in Boulder, Colorado. The authors gratefully acknowledge very helpful discussions on aspects of this work with Drs. John Finnigan and Michael Raupach, both of CSIRO, Canberra, Australia. Last but not least, the first author is indebted to George Thurtell for teaching him the scientific method, and for more than three decades of inspiration and encouragement.

References

Deardorff, J.W., 1980. Stratocumulus-capped mixed layers derived from a three-dimensional model. Boundary-Layer Meteorol. 18, 495–527.

Denmead, O.T., Bradley, E.F., 1985. On scalar transport. In: Hutchison, B.A., Hicks, B.B. (Eds.), Plant Canopies: The Forest–Atmosphere Interaction. Reidel, Dordrecht, pp. 421–442.

Dwyer, M.J., Patton, E.G., Shaw, R.H., 1997. Turbulent kinetic energy budgets from a large-eddy simulation of airflow above and within a forest. Boundary-Layer Meteorol. 84, 23–43.

Finnigan, J.J., 1979. Turbulence in waving wheat. Part II. Structure of momentum transfer. Boundary-Layer Meteorol. 16, 213–236.

Finnigan, J.J., 1985. Turbulent transport. In: Hutchison, B.A., Hicks, B.B. (Eds.), Flexible Plant Canopies: The Forest–Atmosphere Interaction. Reidel, Dordrecht, pp. 443–480.

Gao, W., Shaw, R.H., Paw, U.K.T., 1989. Observation of organized structure in turbulent flow within and above a forest canopy. Boundary-Layer Meteorol. 47, 349–377.

Kanda, M., Hino, M., 1994. Organized structures in developing turbulent flow within and above a plant canopy, using a large eddy simulation. Boundary-Layer Meteorol. 68, 237–257.

Moeng, C.-H., 1984. A large-eddy simulation model for the study of planetary boundary-layer turbulence. J. Atmos. Sci. 41, 2052–2062.

Moeng, C.-H., Wyngaard, J.C., 1988. Spectral analysis of large-eddy simulations of the convective boundary layer. J. Atmos. Sci. 45, 3573–3587.

Patton, E.G., Shaw, R.H., Judd, M.J., Raupach, M.R., 1998. Large-eddy simulation of windbreak flow. Boundary-Layer Meteorol. 87, 275–306.

Raupach, M.R., 1981. Conditional statistics of Reynolds stress in rough-wall and smooth-wall turbulent boundary layers. J. Fluid Mech. 108, 363–382.

Raupach, M.R., Shaw, R.H., 1982. Averaging procedures for flow within vegetation canopies. Boundary-Layer Meteorol. 22, 79–90.

Schlicting, H., 1968. Boundary-Layer Theory. McGraw-Hill, New York, p. 747.

Shaw, R.H., Schumann, U., 1992. Large-eddy simulation of turbulent flow above and within a forest. Boundary-Layer Meteorol. 61, 47–64.

Shaw, R.H., Seginer, I., 1985. The dissipation of turbulence in plant canopies. In: Proceedings of the 7th Symposium of the American Meteorological Society on Turbulence and Diffusion. Boulder, Colorado, pp. 200–203.

Shaw, R.H., Tavangar, J., Ward, D.P., 1983. Structure of the Reynolds stress in a canopy layer. J. Climate Appl. Meteorol. 22, 1922–1932.

Shaw, R.H., den Hartog, G., Neumann, H.H., 1988. Influence of foliar density and thermal stability on profiles of Reynolds stress and turbulence intensity in a deciduous forest. Boundary-Layer Meteorol. 45, 391–409.

Su, H.-B., Shaw, R.H., Paw, U.K.T., Moeng, C.-H., Sullivan, P.P., 1998. Turbulent statistics of neutrally stratified flow within and above a sparse forest from large-eddy simulation and field observations. Boundary-Layer Meteorol. 88, 363–397.

Su, H.-B., Shaw, R.H., Paw, U.K.T., 2000. Turbulent statistics of neutrally stratified flow within and above a sparse forest from large-eddy simulation and field observations. Boundary-Layer Meteorol. 88, 363–397.

Sullivan, P.P., McWilliams, J.C., Moeng, C.-H., 1996. A grid nesting method for large-eddy simulation of planetary boundary layer flows. Boundary-Layer Meteorol. 80, 167–202.

Thorn, A.S., 1971. Momentum absorption by vegetation. Q. J. R. Meteorol. Soc. 97, 414–428.

Wilson, N.R., Shaw, R.H., 1977. A higher-order closure model for canopy flow. J. Appl. Meteorol. 16, 1197–1205.

Wilson, J.D., 1988. A second-order model for flow through vegetation. Boundary-Layer Meteorol. 42, 371–392.